Brain Structure and Function (2019) 224:2757–2774
https://doi.org/10.1007/s00429-019-01934-5

ORIGINAL ARTICLE

Origin of acoustic–vestibular ganglionic neuroblasts in chick embryos and their sensory connections

Luis Óscar Sánchez-Guardado[1] · Luis Puelles[2,3] · Matías Hidalgo-Sánchez[1]

Received: 7 February 2019 / Accepted: 31 July 2019 / Published online: 8 August 2019

Abstract

The inner ear is a complex three-dimensional sensory structure with auditory and vestibular functions. It originates from the otic placode, which generates the sensory elements of the membranous labyrinth and all the ganglionic neuronal precursors. Neuroblast specification is the first cell differentiation event. In the chick, it takes place over a long embryonic period from the early otic cup stage to at least stage HH25. The differentiating ganglionic neurons attain a precise innervation pattern with sensory patches, a process presumably governed by a network of dendritic guidance cues which vary with the local micro-environment. To study the otic neurogenesis and topographically-ordered innervation pattern in birds, a quail–chick chimaeric graft technique was used in accordance with a previously determined fate-map of the otic placode. Each type of graft containing the presumptive domain of topologically-arranged placodal sensory areas was shown to generate neuroblasts. The differentiated grafted neuroblasts established dendritic contacts with a variety of sensory patches. These results strongly suggest that, rather than reverse-pathfinding, the relevant role in otic dendritic process guidance is played by long-range diffusing molecules.

Keywords Developing inner ear · Otic placode · Neuroblast · Sensory patch · Maculae · Cristae · Otic innervation

Introduction

The initial morphological sign of incipient inner ear development is the formation of the otic placodes as thickened portions of the cephalic ectoderm on both sides of the developing hindbrain. These extend longitudinally from rhombomere 4 to pro-rhombomere C levels in birds (Sánchez-Guardado et al. 2014). Cell fate specification and morphogenesis of the placode seem orchestrated by diffusible molecules released from nearby tissues and the otic epithelium itself. This signalling network leads to the differentiation at specific locations of various sensory and non-sensory patches in the developing membranous labyrinthine wall, a process that also underlies the specification of the derived sensory neuroblasts which migrate a short distance away from the otic epithelium into the underlying mesenchyme to create the acoustic–vestibular ganglion (AVG) (Bok et al. 2007; Fekete and Campero 2007; Schneider-Maunoury and Pujades 2007; Whitfield and Hammond 2007; Groves and Fekete 2012; Wu and Kelley 2012; Chen and Streit 2013; Lassiter et al. 2014; Raft and Groves 2015; Alsina and Whitfield 2017).

Neuroblast specification is the first cell differentiation event occurring in the developing vertebrate inner ear (Carney and Silver 1983; Alvarez et al. 1989; Hemond and Morest 1991; Ma et al. 1998, 2000; Fariñas et al. 2001; Alsina et al. 2004, 2009; Abello and Alsina 2007) *Neurogenin1* (*neurog1*), a neural-specific basic Helix–Loop–Helix (bHLH) transcription factor, is expressed in the placodal ectoderm prior to the onset of neuroblast delamination. It is required for the differentiation of proximal cranial sensory neurons, which are completely absent in *neurog1* null mutants, for sensory neuron projections to the inner ear (Ma

Electronic supplementary material The online version of this article (https://doi.org/10.1007/s00429-019-01934-5) contains supplementary material, which is available to authorized users.

✉ Matías Hidalgo-Sánchez
mhidalgo@unex.es

[1] Department of Cell Biology, School of Science, University of Extremadura, E06071 Badajoz, Spain

[2] Department of Human Anatomy and Psychobiology, School of Medicine, University of Murcia, E30100 Murcia, Spain

[3] Instituto Murciano de Investigaciones Biosanitarias (IMIB-Arrixaca), E30100 Murcia, Spain

et al. 1998, 2000; Matei et al. 2005), and for the activation of genes as *NeuroD*, *Atoh1* and the Delta/Notch signalling pathway, which together determine an irreversible commitment of otic neurons (Ma et al. 1998; Abelló et al. 2007; Alsina et al. 2009; Yang et al. 2011; Coate and Kelley 2013; Gálvez et al. 2017). *Sox2*, *Fgf19* and *Prox1*, among other genes, are also involved in fate specification and neurogenesis (Stone et al. 2003; Sanchez-Calderon et al. 2007a, b; Alsina et al. 2009; Puligilla et al. 2010; Wu and Kelley 2012; Dvorakova et al. 2016; Gálvez et al. 2017).

The subsequent dendritic ganglionic innervation of hair cells of developing sensory patches is carried out by ganglionic neurons (Kawamoto et al. 2003; Fritzsch 2003; Beisel et al. 2005; Fekete and Campero 2007; Fritzsch et al. 2015; Delacroix and Malgrange 2015; Zhang and Coate 2017). These neurons ultimately project their axons to the segmentally organised acoustic and vestibular sensory nuclei of the hindbrain (Fritzsch et al. 2002; Maklad and Fritzsch 2003; Maklad et al. 2010; Mahmoud et al. 2013; Straka and Baker 2013; Elliott and Fritzsch 2018; see also refs. therein). Despite the abundance of descriptive and experimental studies on the specification of areas of neurogenesis (Liu et al. 2000; Rubel and Fritzsch 2002; Stone et al. 2003; Sanchez-Calderon et al. 2007a; Koundakjian et al. 2007; Alsina et al. 2009; Dyballa et al. 2017) and the subsequent orderly dendritic connection (Rubel and Fritzsch 2002; Fekete and Campero 2007; Holt et al. 2011; Simmons et al. 2011; Coate and Kelley 2013; Mao et al. 2014; Lassiter et al. 2014; Raft and Groves 2015; Coate et al. 2015; Meas et al. 2018), some aspects of the molecular and cellular mechanisms involved still call for further investigation to better understand these developmental events.

It has been suggested that the complex ordered innervation of the diverse acoustic and vestibular sensory epithelia by maturing ganglionic neurons may be governed by a code of dendritic guidance cues acting at key decision points (Rubel and Fritzsch 2002; Fritzsch 2003; Fekete and Campero 2007). Several specific hypotheses have been proposed to explain the mechanisms guiding the leading processes of apparently mixed populations of differentiating neuroblasts towards specific sensory epithelia in the developing otic rudiment. A "reverse-pathfinding" mechanism was suggested by which, as ganglionic neuroblasts migrate out of the placode, each subset of neuroblasts would define the future substrate pathway for its dendrites, leaving a molecular trail to the sensory patch. The pioneering dendrites of these neuroblasts would just follow these paths backwards, thus creating topographically ordered innervation patterns which are precise with respect to specific sensory targets (Carney and Silver 1983). This assumption necessarily implies that all developing sensory epithelia generate their own neuroblasts, and predict a clonal relationship between subgroups of ganglionic neurons and their sensory targets. However, it was later noted that some neuroblasts do not delaminate from the same site of the developing otic epithelium which they will later innervate (Noden and van de Water 1986). The first neuroblasts are known to emerge from the anteromedial half of the otic primordium (Carney and Silver 1983; Alsina et al. 2004, 2009; Bell et al. 2008). Furthermore, the area from which all *neurotrophin*/*NeuroD*-positive ganglionic neuroblasts delaminate corresponds exclusively to the presumptive domains of the utricular and saccular maculae (Raft et al. 2007). Accordingly, the rest of the developing sensory patches would not generate any migrating neuroblasts, thus reducing the heuristic weight of the reverse-pathfinding hypothesis. Nevertheless, studies using proneuronal gene promoters and innovative labelling approaches have suggested that additional sites of neuronal specification gradually emerge within the developing otic epithelium, with otic neuroblasts eventually delaminating from all of them. In the mammalian developing inner ear, there have been direct demonstrations of delaminating neuroblasts coming from specific areas, rather than uniformly, along the growing cochlear duct (Fariñas et al. 2001; Matei et al. 2005; Yang et al. 2011). One may conclude from these results that at least the developing utricle, saccule and cochlear duct generate neuroblasts. Consequently, the hypothesis suggests itself that genetically differentiated neurons are generated which potentially carry differential molecular profiles.

In addition to this line of thought, some other studies instead suggest the hypothesis that the sensory epithelial patches might release specific chemoattractant molecules which attract the growth cones of subsets of AVG neurons during the dendritic guidance period (Hemond and Morest 1991, 1992; Bermingham et al. 1999; Stevens et al. 2003; Fritzsch et al. 2004). Nevertheless, the particular molecular mechanisms involved in the accurate innervation pattern of sensory patches by differentiated neurons remain an open question (Rubel and Fritzsch 2002; Xiang et al. 2003; Pauley et al. 2003; Fritzsch et al. 2005; Fekete and Campero 2007).

With the intention of exploring this long-standing issue, we performed an experimental study using the quail/chick chimaeric graft method. With the experience accruing from our previous fate mapping study (Sánchez-Guardado et al. 2014), we transplanted small portions of the otic placode containing the presumptive territory of specific sensory patches, conjointly with small portions of nearby prospective non-sensory epithelium, in which ganglionic neurons may arise. (We shall refer to such mixed grafts as "expanded presumptive sensory areas"). Then we analysed the pattern of QCPN-positive grafted ganglionic neuroblasts and were able to conclude that all grafted expanded sensory areas generate neuroblasts. By means of QN-immunoreactive labelling of the processes of graft-derived quail ganglionic neurons (Tanaka et al. 1990), we were able to determine the patterns of their connections with sensory area-derived receptor

patches. From this analysis, we shall conclude that ganglionic neuroblasts originating from grafted small expanded presumptive sensory areas of the chick otic placode in the period analysed (HH10-HH36) do not project to the correlative grafted sensory area exclusively, but also innervate many other topologically distant sites. The data are, thus, more consistent with the conjecture of a diversity of long-range diffusible signals than with the simple "reverse-path-finding" mechanism.

Materials and methods

Tissue processing

Fertilised White Leghorn chick (*Gallus gallus*) and Japanese quail (*Coturnix coturnix japonica*) eggs were incubated in a humidified atmosphere at 38 ± 1 °C. Avian chimaeric embryos were fixed and processed for cryostat sections as previously described (Sánchez-Guardado et al. 2009).

Grafting experiments

Chick and quail embryos were used to obtain chimaeras by exchanging specific portions of the cephalic ectoderm adjacent to the hindbrain at the 10-somite stage [HH10, (Hamburger and Hamilton 1992)] in unilateral homotopic and isochronic transplants. Six types of transplants were carried out (Fig. 1a, b). These grafting experiments were planned in accordance with the recent fate mapping study of the chick otic placode (Sánchez-Guardado et al. 2014). The constrictions between neighbouring hindbrain rhombomeres or pro-rhombomeres served as positional landmarks (see Vaage 1969). A grid inserted into one ocular of the operating microscope helped to identify the relative position of the presumptive domain of each sensory and non-sensory element of the avian inner ear according to either the anterior–posterior or mediolateral axes of the otic placode at the 10-somite stage. To prevent any contribution of the hindbrain and neural crest to the inner ear (D'Amico-Martel and Noden 1983; Freyer et al. 2011), the grafted territories were exclusively restricted to a small portion of the otic placode (Fig. 1c). The in ovo micro-surgical procedure was that described in detail by (Alvarado-Mallart and Sotelo 1984). Chick embryos (always the hosts) were operated on in ovo. For these in ovo operations, a small window was made in the shell. Black ink diluted in phosphate buffer was then injected into the yoke under the embryo to improve the latter's visualisation. Quail embryos were always used as donors. They were excised and removed from the eggs using fine scissors, then put into phosphate buffer and pinned onto black wax. A cavity was prepared in the chick otic placode to receive the quail graft. For this purpose, the constrictions

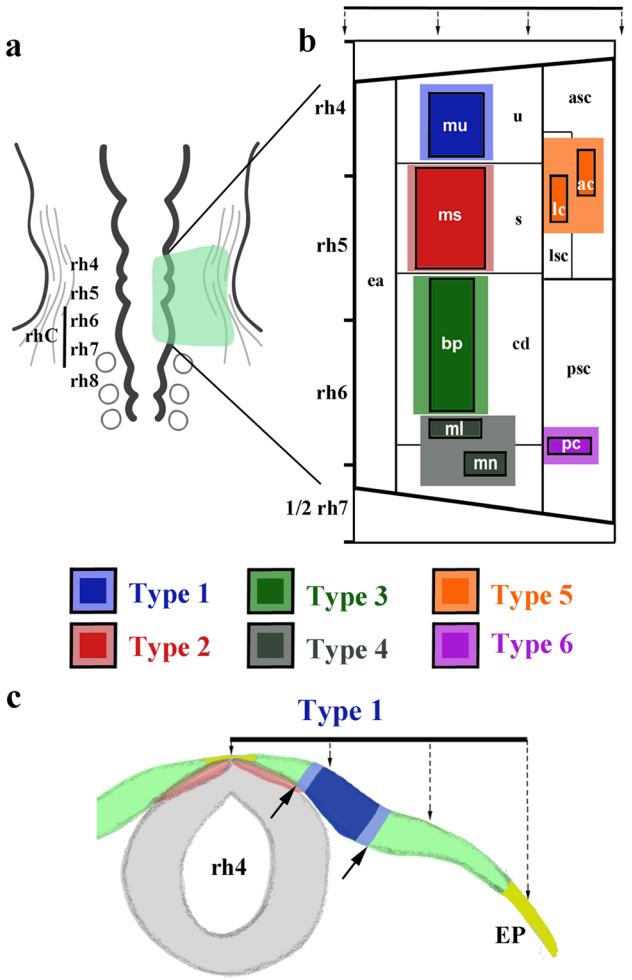

Fig. 1 Schematic representation of quail–chick grafting experiments at the 10-somite stage. **a** Schematic dorsal view of an avian embryo showing the otic placode in the cephalic ectoderm, facing rhombomeres (rh) rh4, rh5, and a large part of rhC which will soon after be subdivided into rh6 and rh7 (see Vaage 1969). **b** Six types of grafts were performed, termed here as "expanded sensory areas", estimated to contain the presumptive territory of specific sensory patches (dark colour) together with small portions of nearby prospective non-sensory epithelium (light colour), in accordance with (Sánchez-Guardado et al. 2014). **c** Schematic transverse section through the otic placode at the level of rh4 showing the Type 1 graft (light and dark blue; between arrows in **c**). The grafted territories affected exclusively a small portion of the otic placode, preventing any contribution of the hindbrain and other embryonic epithelial structures close to the otic placode. The dotted lines in **b** and **c** indicate the three subdivisions considered in a previous fate mapping study (Sánchez-Guardado et al. 2014). *ac* anterior crista, *asc* anterior semicircular canal, *bp* basila papilla, *EP* epidermis, *ea* endolymphatic apparatus, *lc* lateral crista, *lsc*, lateral semicircular canal, *ml* macula lagena, *mn* macula neglecta, *ms* macula sacculi, *mu* macula utriculi, *pc* posterior crista, *psc* posterior, semicircular canal, *rh* rhombomere, *s* saccule, *tv* tegmentum vasculosum, *u* utricle

between rhombomeres and the grid inserted into one ocular helped us very precisely create the appropriate cavity using custom hand-made micro-scalpels—stainless steel needles

with a thickness of 0.1–0.2 mm glued to a toothpick. The graft was prepared in parallel by excising the same area of the quail otic placode. It was then transported in a glass micropipette for placement into the corresponding cavity of the host. Particular care was taken for the sizes of the cavity and the graft in the otic placode to be closely matched for the successful integration of the transplant. In particular, chimaeric embryos with different sizes of cavity and graft were discarded. After transplantation, the host eggs were closed with Parafilm, sealed with paraffin, and kept at 38 ± 1 °C. The resulting chimaeric embryos were analysed at 10 days of incubation (stage HH36) when major morphogenetic changes have already taken place and all sensory elements are completely innervated (Sánchez-Guardado et al. 2013). About 180 chimaeric embryos were analysed. Any experimental embryos with a quail graft different from that which was planned or containing structures outside the otic placode, such as portions of the very close cranial placodes, were discarded. The number of grafts performed in each experiment is indicated in the corresponding sections of Results and Figure Legends.

Immunohistochemical staining procedure

QCPN (DSHB; 1/100) and QN mAb (1/10, a kind gift from Dr Tanaka) antibodies were used to visualise the bodies and processes of grafted cells, respectively. For this visualisation, sheep anti-mouse (1/100; Jackson ImmunoResearch) and mouse-PAP (1/200; Jackson ImmunoResearch) antibodies were used. Histochemical detection of peroxidase activity was carried out using 0.03% DAB with 0.6% nickel ammonium sulphate and 0.005% H_2O_2.

Imaging and quantification

All preparations were photographed with a Zeiss Axiophot microscope equipped with a Zeiss AxioCam camera (Carl Zeiss, Oberkochen, Germany) and AxioVision 2.0.5.3. software, and the images were saved in 4-MB TIFF format. These were size adjusted, cropped, contrast enhanced and annotated with Adobe Photoshop version 7.0 software (Adobe Systems, San Jose, CA). A quantitative study was performed with NIS Elements Imaging software. The percentage of the area of each mature sensory patch innervated by grafted neurons with respect to its whole area was calculated in the six experimental types. Three qualitative groups were considered to indicate the relative amount of innervation. "Few" QN-stained axons detected in a sensory element correspond to an innervated area of 1–33% and are represented with one asterisk. "Moderate" QN-positive dendrites correspond to 34–66% and are illustrated with two asterisks. "Many" QN-stained dendrites correspond to 67–100% and are shown with three asterisks. Three, two and one asterisks correspond to thick, intermediate and thin arrows, respectively, which are shown in separate figures for each grafted region (Figs. 4l, 5m, 6l, 7m, 8m, 9g). When less than three QN-stained axons were detected within a sensory patch, a thin broken line was used (Fig. 9g). Table 1 is a synthesis of

Table 1 Overall summary of all types of experiments, indicating the homotopically grafted placodal areas and the sensory patches to which the correlative grafted neuroblasts projected

		Innervated sensory patch									
		mu	ms	ac	lc	*p*-bp	*i*-bp	*d*-bp	ml	mn	pc
Grafted area											
mu	Type 1 $n=9$	83 ± 7***	89 ± 6***	44 ± 4**	40 ± 3**	79 ± 4***	85 ± 5***	43 ± 7**	46 ± 4**	39 ± 7**	53 ± 7**
ms	Type 2 $n=9$	92 ± 3***	83 ± 6***	71 ± 6***	72 ± 5***	0 ± 0	4 ± 2*	36 ± 7**	73 ± 7***	77 ± 8***	87 ± 5***
bp	Type 3 $n=8$	81 ± 4***	73 ± 4***	10 ± 3*	40 ± 5**	0 ± 0	9 ± 9*	48 ± 7**	49 ± 5**	70 ± 3***	74 ± 4***
ml/mn	Type 4 $n=8$	27 ± 6*	24 ± 4*	14 ± 5*	26 ± 7*	0 ± 0	0 ± 0	40 ± 7**	45 ± 3**	35 ± 9**	76 ± 7***
ac/lc	Type 5 $n=7$	8 ± 2*	71 ± 6***	76 ± 5***	23 ± 3*	0 ± 0	**	**	*	18 ± 3*	30 ± 5*
pc	Type 6 $n=6$	0 ± 0	1 ± 0^+	7 ± 1*	1 ± 0^+	0 ± 0	0 ± 0	0 ± 0	0 ± 0	0 ± 0	5 ± 1*

The percentage of the area of each mature sensory patch innervated by grafted neurons with respect to its whole area was calculated in each experimental type. The number of asterisks indicates the relative quantity of QN-positive processes reaching each sensory element: ***, many (an innervated area of 67–100%); **, a moderate number (an innervated area of 34–66%); *, few (an innervated area of 1–33%); $^+$, occasional processes observed in some embryos. This asterisk code corresponds to the arrow thicknesses used in the summarising diagrams of Figs. 1, 2, 3, 4, 5 and 6 (***, thick arrow; **, intermediate thickness arrow; *, thin arrow, +, thin broken line). The arithmetic mean and the standard deviation, as well as the number of grafts of each type, are indicated

the results for all the chimaeric embryos analysed, covering from Type 1 to Type 6 experiments, including a quantitative study concerning the arithmetic mean and the standard deviation.

Results

A crucial issue in vertebrate inner ear development is the precise correlation between the topographic origin of ganglionic neuroblasts and their respective later projections to particular sensory patches in the developing membranous labyrinth. To better understand this developmental question, we performed homotopic quail–chick grafts of small portions of the otic placode which included the presumptive territory of given otic sensory areas according to a precise fate map that we had made previously for the 10-somite stage [HH10, (Sánchez-Guardado et al. 2014); Fig. 1a, b]. Since vestibular and auditory ganglionic neurons might be clonally related to non-sensory epithelia (see the "Discussion" below), the quail grafts included a small portion of the non-sensory epithelium lying around the sensory patches considered (Fig. 1b, c). For this reason, we term the grafted tissue, comprising sensory plus adjacent non-sensory epithelium, an "expanded presumptive sensory area". The resulting chimaeric embryos were analysed in horizontal sections at 10 days of incubation (HH36) when the otic innervation pattern has been completely established (Fritzsch 1993; Sánchez-Guardado et al. 2013). This kind of experiment allows one to consider all the neuroblasts generated in a specific grafted area from the time of the transplantation (the otic placode stage, HH10) to the moment when the chimaeric embryos were fixed (HH36). However, this kind of experiment is not suited to determining whether there exists a common progenitor for hair cells and neuroblasts in each sensory patch. In particular, it was left unclear whether, when the grafts generate neuroblasts, the grafted areas were exclusively neurogenic domains or already specified sensory patches. QCPN monoclonal antibody was used to visualise the grafted quail cells in the chick otic epithelium (Sánchez-Guardado et al. 2014). QN monoclonal antibody was used to establish the innervation pattern created by graft-derived neurons (Tanaka et al. 1990).

Type 1–6 expanded placodal grafts generated neuroblasts

To determine whether the grafted area of each type of experiment could generate otic neuroblasts, we first analysed the existence of QCPN-stained grafted quail neurons in horizontal sections through the vestibular ganglia (VG; Fig. 2) and acoustic ganglia (AG; Fig. 3) in all chick/quail chimaeric embryos. They all clearly showed QCPN-stained neurons in the VG (arrows in Fig. 2a–f). QCPN-positive neurons were also generally detected in the AG (arrows in Fig. 3a–e) except in Type 6 experimental embryos, whose AG was completely devoid of QCPN-stained neurons (Fig. 3f).

Neuroblasts derived from the expanded macula utriculi area innervate every sensory patch

When the presumptive placodal territory of the macula utriculi area was included in the stage-HH10 expanded graft (Type 1; mu in Fig. 4a), and the host was immunoreacted with QCPN at stage HH36 to identify the grafted area (Fig. 4b; see S1 Fig.), the graft-derived neuroblasts generated a large number of QN-stained dendrites (Fig. 4c–k). The entire extent of the grafted macula utriculi was innervated by many QN-positive fibres (Fig. 4f). The nearby macula sacculi also showed abundant quail QN-stained dendrites (Fig. 4g). Surprisingly, all ampullary cristae were innervated by fewer QN-positive fibres (Fig. 4c–e, h). The macula neglecta, located close to the posterior crista, also displayed immunoreactive fibres originating from the grafted neurons (Fig. 4h). We analysed as well the innervation pattern of the basilar papilla and the macula lagena in the cochlear duct (Fig. 4i–k). The dorsoventrally arranged basilar papilla showed many QN-stained processes over its entire extent, including its proximal (*p*-bp, Fig. 4i) and distal (*d*-pb, Fig. 4j) portions. Some areas of the distal basilar papilla were devoid of QN-positive axons (Fig. 4j′). The macula lagena, located at the end of the cochlear duct, was innervated by far fewer QN-positive dendrites (Fig. 4k). Figure 4l summarises these results. The size of the arrows represents the relative quantity of QN-positive fibres reaching each sensory element (see also Table 1).

Neuroblasts derived from the expanded macula sacculi area

When the territory of the presumptive macula sacculi area was transplanted (Type 2; ms in Fig. 5a, stage HH10), and the host was examined by QCPN immunoreaction (between arrowheads in Fig. 5b; see S2 Fig.), the QN-positive dendritic processes of graft-derived neurons were also found to reach all sensory patches. All ampullary cristae received QN-stained fibres (ac, lc and pc in Fig. 5c–e, h). There were clearly more of these fibres than when the expanded domain of the presumptive macula utriculi was grafted (Type 1; Fig. 4c–e, h). All maculae, including the macula neglecta and macula lagena, likewise presented many quail-derived dendritic processes (mu, Fig. 5f; ms, Fig. 5g; mn, Fig. 5h; ml, Fig. 5l). The macula lagena showed more QN-stained fibres in Type 2 than in Type 1 grafts (compare Fig. 4k and Fig. 5l). With respect to the basilar papilla, its distal portion also displayed abundant QN-positive fibres, but less dendrites

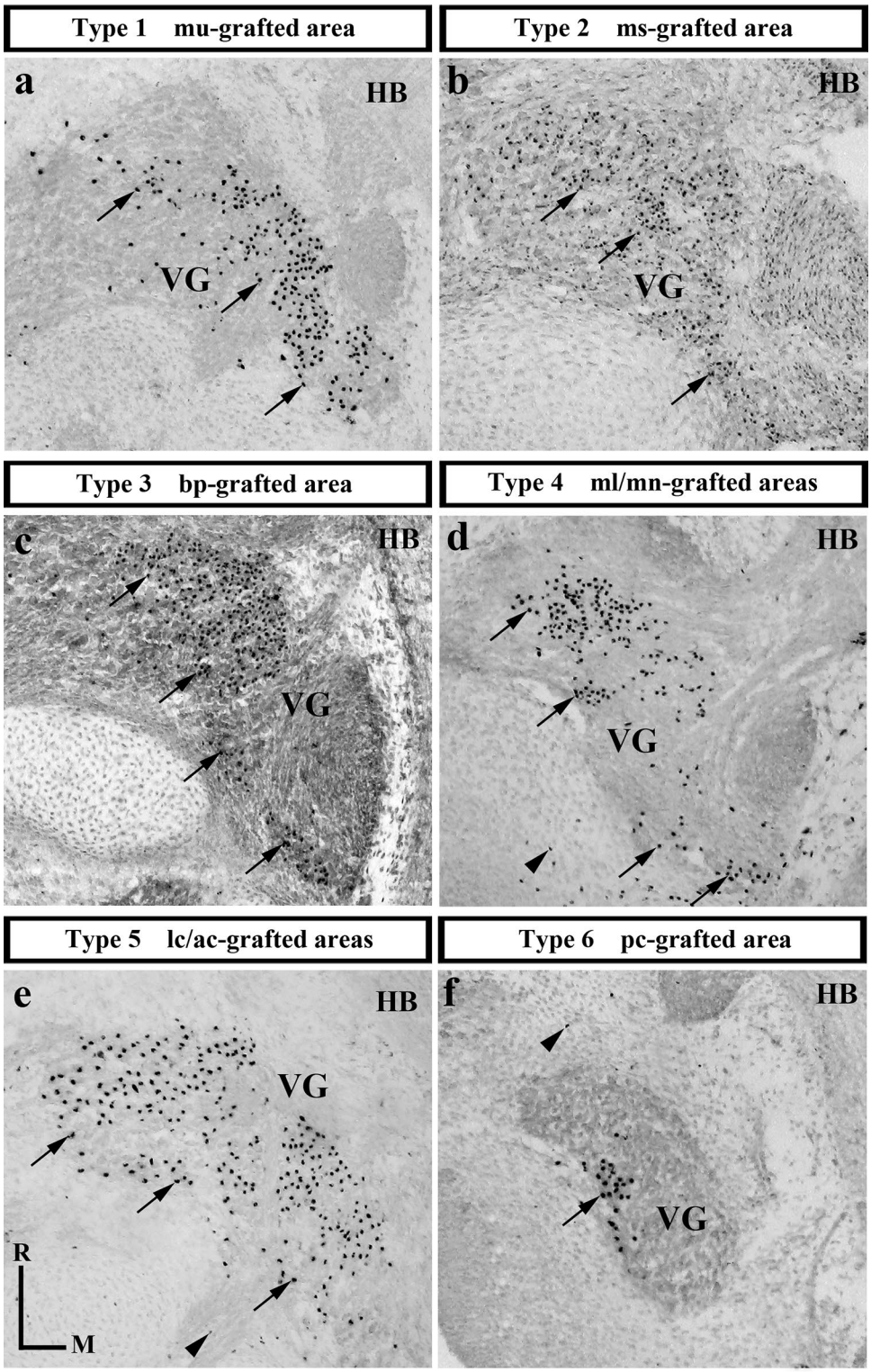

Fig. 2 Graft-derived quail ganglionic neurons in the vestibular ganglion (VG). QCPN-stained grafted quail neurons (arrows in **a**–**f**) are clearly present in horizontal sections through the VG of all our chimaeric embryos (Types 1–6 in Fig. 1**b**). The larger size of the ganglionic neurons differentiated from the grafted otic epithelium (arrows) easily allows them to be distinguished from mesenchymal cells included in the graft (arrowheads). *A* anterior, *bp* basilar papilla, *cd* cochlear duct, *HB* hindbrain, *M* medial, *R* rostral

than Type1 graft (*d*-bp, Fig. 5k). Its intermediate portion showed a few QN-stained processes in its anterior part (*i*-bp, Fig. 5j), whereas its proximal portion was completely devoid of labelled cell processes (*p*-bp, Fig. 5i). The innervation patterns in the basilar papilla were clearly different in Type 1 and Type 2 experiments (compare Fig. 4i, j with Fig. 5i–k). Figure 5m summarises these results (see also Table 1).

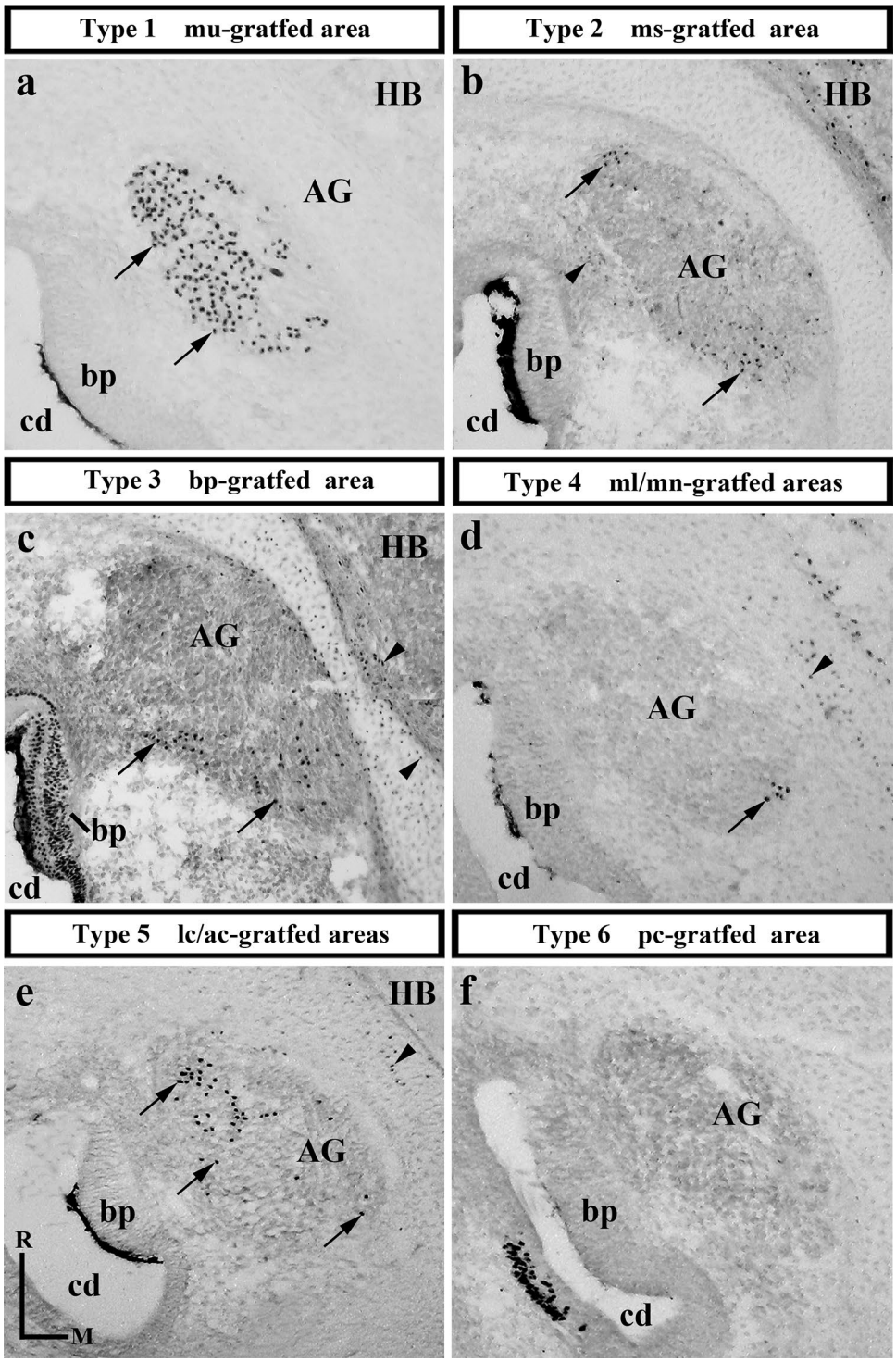

Fig. 3 Graft-derived quail ganglionic neurons in the acoustic ganglion (AG). QCPN-stained grafted quail neurons (arrows in **a**–**f**) were present in the AG in horizontal sections through all our Type 1–5 chimaeric embryos (**a**–**e**). In contrast, the AG of Type 6 experimental embryos were devoid of QCPN-stained neurons (**f**). The arrowheads point to QCPN-stained mesenchymal cells. *A* anterior, *bp* basilar papilla, *cd* cochlear duct, *HB* hindbrain, *M* medial, *R* rostral

Neuroblasts derived from the expanded basilar papilla area

When the expanded basilar papilla area was transplanted (Type 3; bp in Fig. 6a), the QCPN-stained grafts included proximal and distal portions of this sensory area (*p*-bp and *d*-bp; between arrowheads in Fig. 6b; see S3 Fig.). Quail neurons derived from this grafted expanded sensory area also innervated all otic sensory patches, although the number of QN-labelled fibres varied among those patches (Fig. 6c–k). With regard to the ampullary cristae, the lateral and posterior cristae showed a substantial number of QN-positive fibres (lc and pc, Fig. 6d, e, h), whereas the anterior crista showed just a few QN-stained processes (Fig. 6c, c′). All maculae displayed abundant QN-labelled

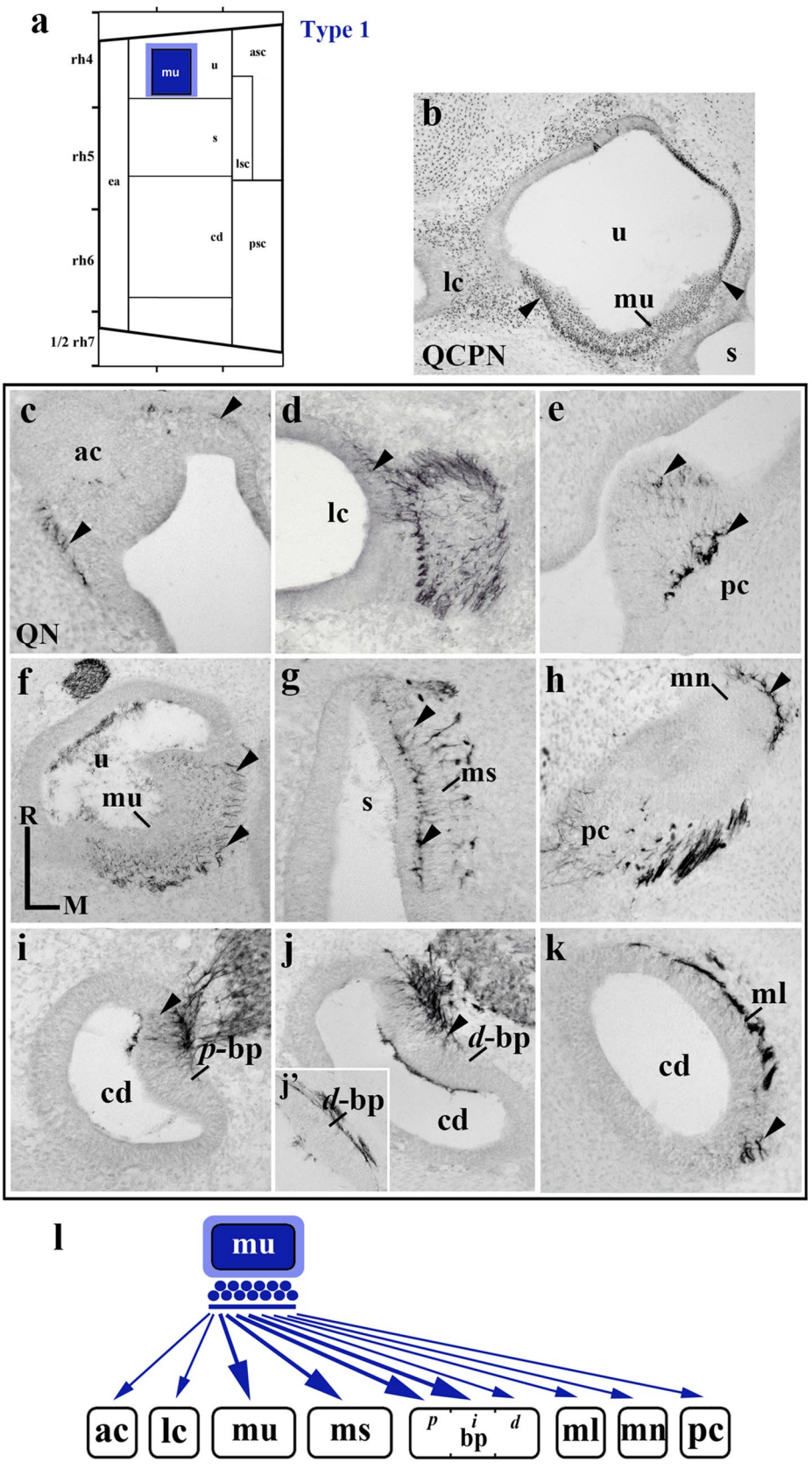

Fig. 4 Labelling obtained from the expanded macula utriculi area. **a** Schematic representation of the Type 1 experiment at the 10-somite stage, involving the macula utriculi area ($n = 9$). **b–k** Horizontal sections through a representative Type 1 chimaeric embryo at 10 days of incubation (E10). The antibodies used are indicated in each panel. The grafted quail sensory cells were detected exclusively in the macula utriculi area (between arrowheads in **b**). QN-positive dendritic fibres from related labelled ganglion cells were detected in all sensory patches (arrowheads; ac, **c**; lc, **d**, pc, **e**, **h**; mu, **f**; ms, **g**; mn, **h**; bp, **i**, **j**; ml, **k**). Regarding the maculae, the utricular and saccular maculae (**f**, **g**) received more QN-stained processes than the rest (mn, **h**; ml, **k**). The entire basilar papilla was innervated by grafted afferent neurons (bp; **i, j**). **l** Diagram summarising all these results. To illustrate qualitatively the number of QN-stained processes, a thick arrow means an abundant number, an intermediate arrow means a moderate number and a thin arrow means a small number. *M* medial, *R* rostral, *cd* cochlear duct, *d-bp* distal basilar papilla, *p-bp* proximal basilar papilla, *u* utricle, *s* saccule

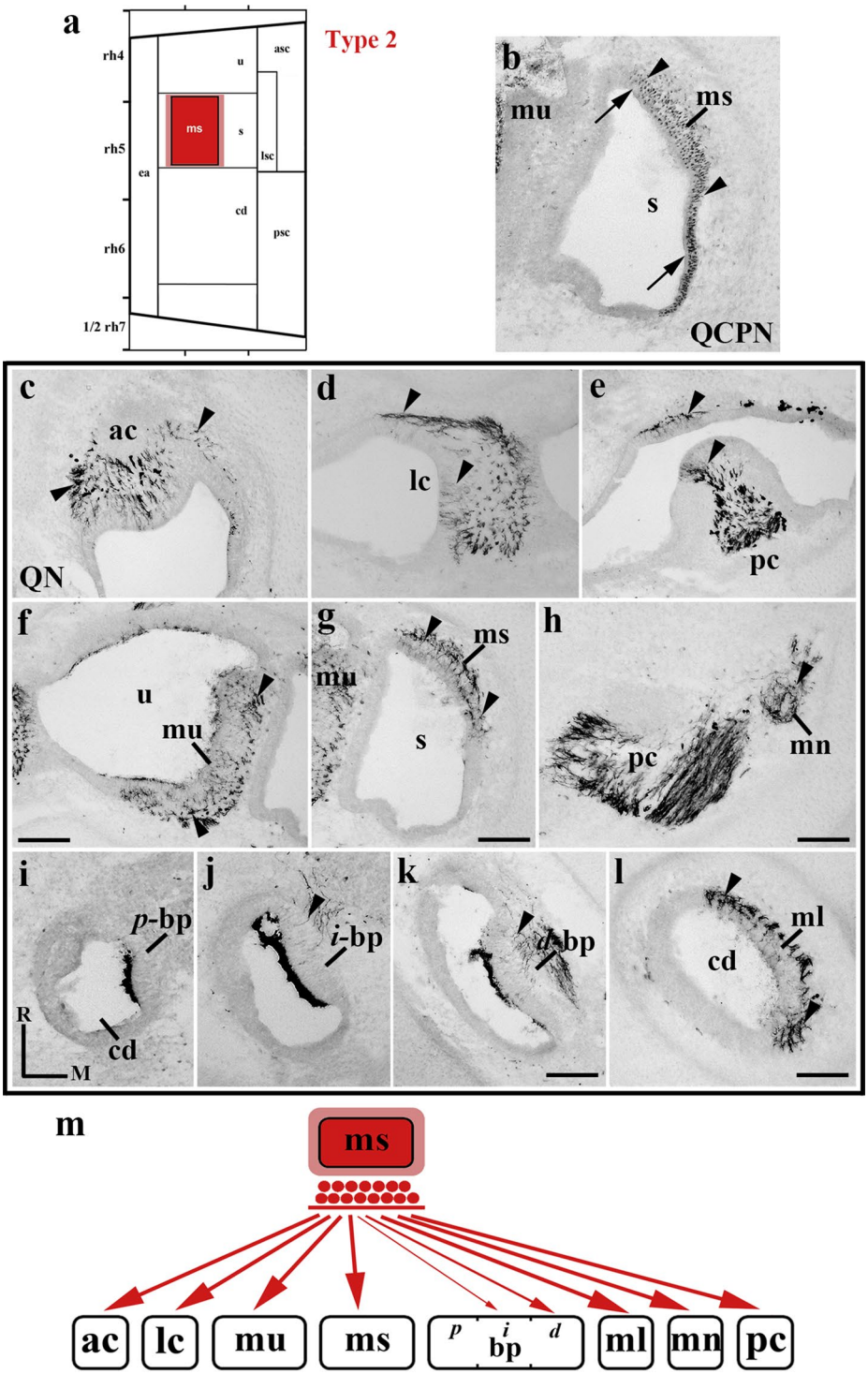

Fig. 5 Labelling obtained from the expanded macula sacculi area. **a** Schematic representation of the Type 2 experiment at the 10-somite stage involving the macula sacculi area ($n=9$). **b–k** Horizontal sections through a Type 2 chimaeric embryo at E10. The grafted quail cells were detected exclusively in the macula sacculi area (between arrowheads in **b**). QN-positive fibres were clearly detected in all sensory patches (arrowheads; ac, **c**; lc, **d**, pc, **e**, **h**; mu, **f**; ms, **g**; mn, **h**; bp, **i-k**; ml, **l**). All cristae and maculae received a high number of QN-stained fibres (**c–h, l**). Regarding the basilar papilla (bp), the intermediate and distal portions were innervated by grafted afferent neurons (*i*-bp and *d*-bp; **j, k**), but not the proximal basilar papilla (*p*-bp; **i**). **m** Diagram summarising all these results. Same code as in Fig. 2l. *M* medial, *R* rostral

processes (mu, ms, mn and ml in Fig. 6f–h, k). The basilar papilla (Fig. 6i, j) presented many QN-positive dendrites, restricted mainly to its distal portion (*d*-bp, Fig. 6j), whereas its intermediate portion received far fewer labelled innervations in its posterior part (*i*-bp, arrowhead in Fig. 6i, i′). The proximal basilar papilla was entirely devoid of QN-stained fibres (not shown). Figure 6l summarises these results (see also Table 1).

Neuroblasts derived from the expanded macula lagena and macula neglecta areas

The Type 4 graft included the presumptive areas of both the macula lagena and the neighbouring macula neglecta (Fig. 7a, Sánchez-Guardado et al. 2014; between arrowheads in Fig. 7b, c; see S4 Fig.). In these grafts, derived

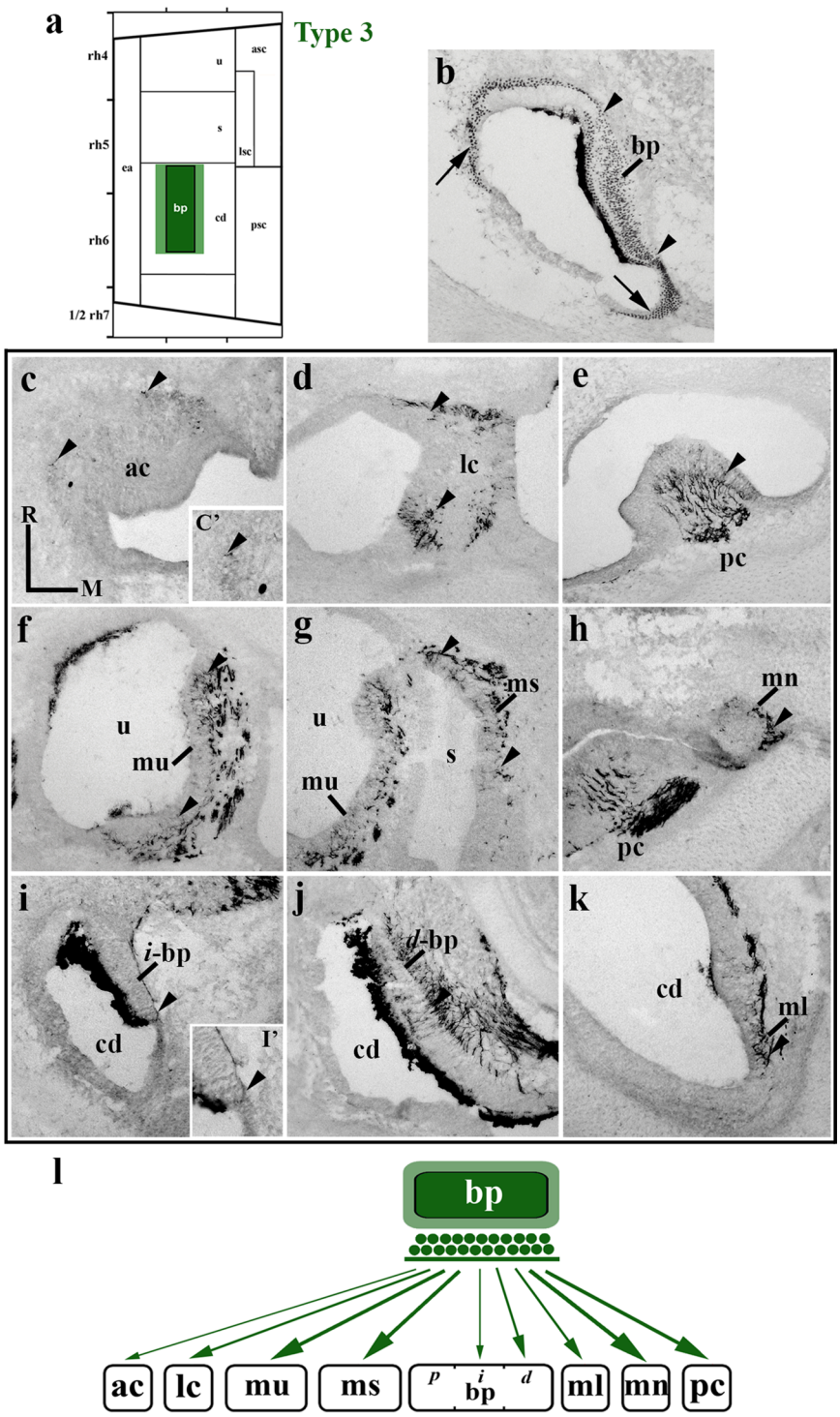

Fig. 6 Labelling obtained from the expanded basilar papilla area. **a** Schematic representation of the Type 3 experiment at the 10-somite stage involving the entire basilar papilla area ($n=8$). **b–k** Horizontal sections through a Type 3 chimaeric embryo at E10. Grafted quail cells were detected exclusively in the basilar papilla area (between arrowheads in **b**). Numerous QN-positive dendrites were clearly detected in all sensory patches (arrowheads; ac, **c**, **c′**; lc, **d**; cp, **e**, **h**; mu, **f**; ms, **g**; mn, **h**; *i*-bp, **i, i′**; d-bp, **j**; ml, **k**). The macula lagena seemed to receive fewer QN-stained dendrites (ml, **k**) than the other maculae. The anterior crista and the intermediate basilar papilla showed a small number of QN-positive dendrites (ac, **c**, **c′**; *i*-bp, **i**, **i′**), whereas the proximal basilar papilla was completely devoid of them (not shown). **l** Diagram summarising all these results. *M* medial; *R* rostral

quail neurons were also projected to all sensory patches (Fig. 7d–l), with local differences being detected in the quantity of QN-positive processes. The posterior ampullary crista was profusely innervated (Fig. 7f, i), whereas the anterior and lateral cristae received just a few QN-stained processes (Fig. 7d, d′, e). With regard to the maculae, those of the utricle and saccule were innervated by far fewer graft-derived fibres (mu and ms in Fig. 7g, h) than the maculae neglecta and lagena (mn and ml in Fig. 7i, l). In the basilar papilla, only its distal part was innervated by QN-positive dendrites (compare *d*-bp in Fig. 7k and *i*-bp in Fig. 7j). However, some areas of the distal basilar papilla were devoid of QN-positive axons (Fig. 7k′). Figure 7m summarises these results (see also Table 1).

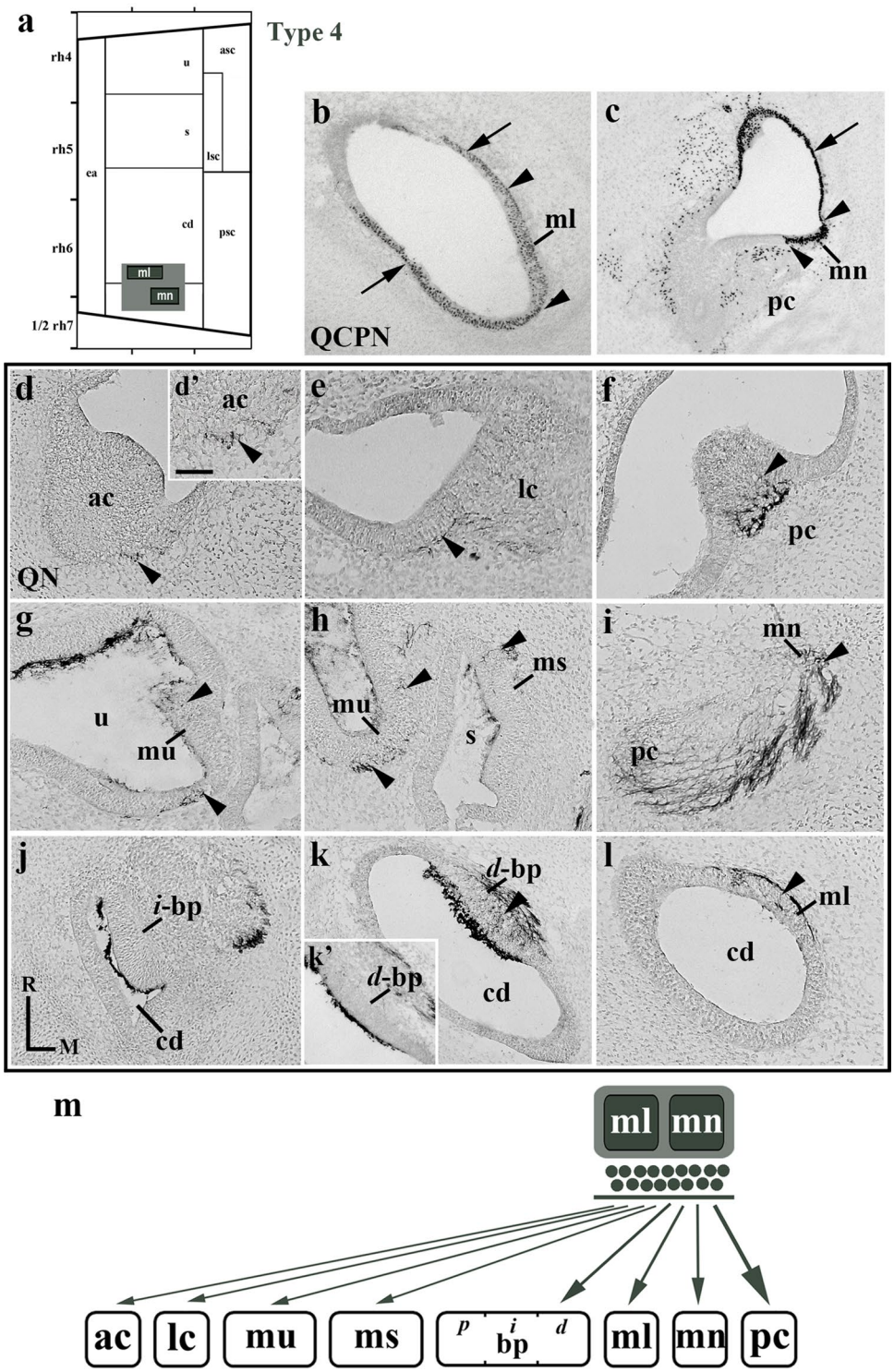

Fig. 7 Labelling obtained from the expanded lagena/neglecta maculae area. **a** Schematic representation of the Type 4 experiment at the 10-somite stage including the macula lagena and macula neglecta areas ($n=8$). **b–l** Horizontal sections through one Type 4 chimaeric embryo at E10. Grafted quail cells were detected in the macula lagena (between arrowheads in **b**) as well as in the macula neglecta (between arrowheads in **c**). QN-positive processes were observed in all sensory patches (arrowheads; ac, **d**, **d′**; lc, **e**; pc, **f**, **i**; mu, **g**, **h**; ms, **h**; mn, **i**; *i*-bp, **j**; *d*-bp, **k**; ml, **l**). The posterior crista (**f**), the macula neglecta (**i**), the distal basilar papilla (*d*-bp, **k**) and the macula lagena (**l**) presented a considerable number of QN-stained dendrites. The anterior and lateral cristae (**d**, **d′**, **e**) and the utricular and saccular maculae (**g**, **h**) displayed very few QN-positive dendrites. The proximal and intermediate portions of the basilar papilla were completely devoid of QN-stained dendrites (see **j** for *i*-bp). **m** Diagram summarising all these results. *M* medial, *R* rostral

Neuroblasts derived from the expanded anterior/lateral area

The fate-mapped domains of the presumptive anterior and lateral ampullary cristae are located at the rostroventral end of the embryonic otic placode (Sánchez-Guardado et al. 2014). Their joint presumptive area was included in one graft experiment type (Type 5; ac and lc in Fig. 8a). In this kind of chimaeric embryo (grafted area between arrowheads in Fig. 8b, c; see S5 Fig.), dendrites of graft-derived neurons abundantly innervated the anterior crista (ac, Fig. 8d), but fewer QN-positive dendrites were observed in the lateral

and posterior cristae (more dendrites reached the lateral crista than the posterior crista; lc and pc in Fig. 8e, e′, f, i). In addition, quail dendrites were observed in the macula utriculi (mu, Fig. 8g) and the macula sacculi (ms, Fig. 8h), while there were few innervating the macula neglecta (mn, Fig. 8i) and macula lagena (ml, Fig. 8l, l′). Interestingly, only the intermediate and distal portions of the basilar papilla presented quail-derived dendrites (*p*-bp, not shown; *i*-bp, Fig. 8j; *d*-bp, Fig. 8k). This innervation was particularly evident in the distal portion (*d*-bp; Fig. 8k). Figure 8m summarises these results (see also Table 1).

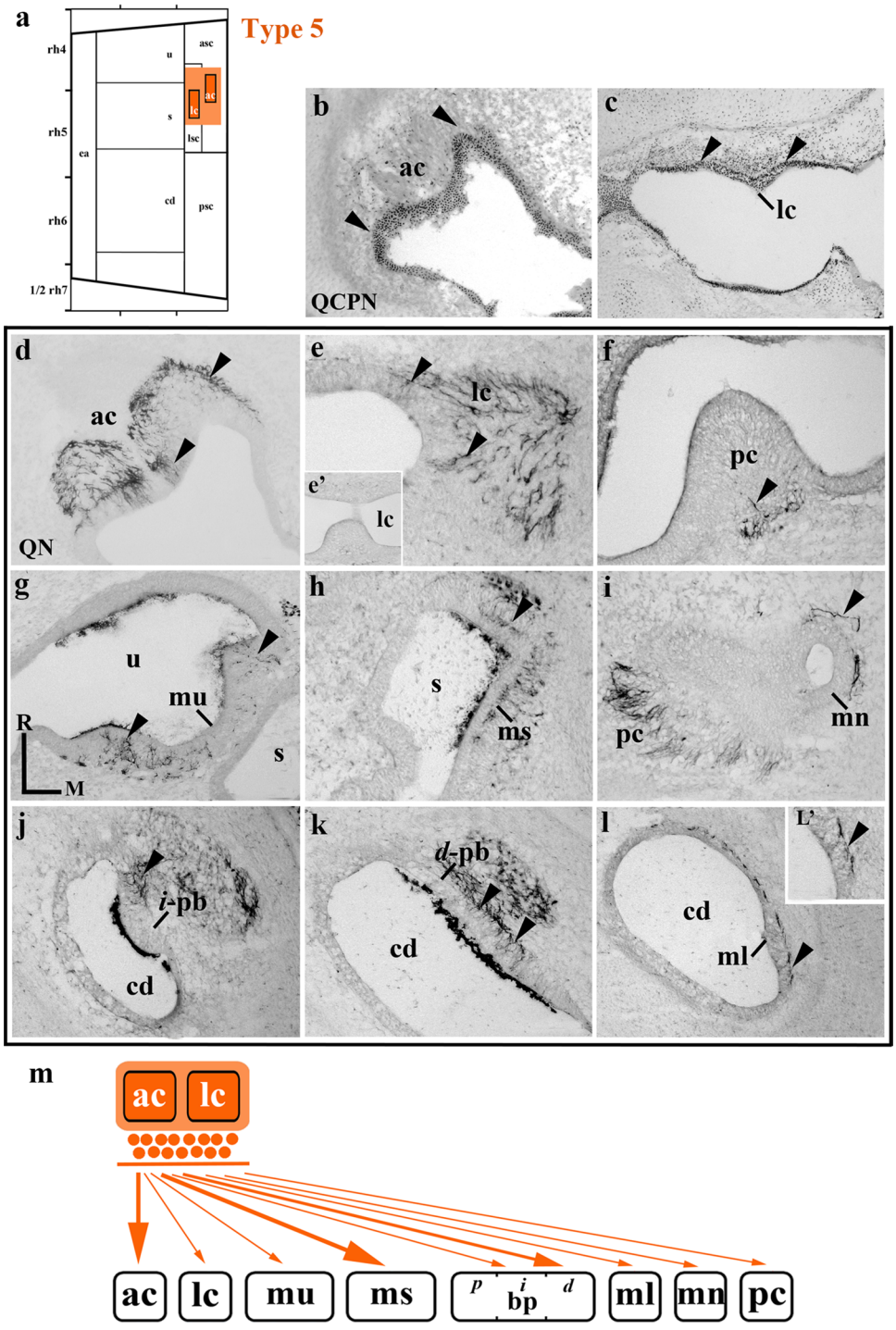

Fig. 8 Labelling obtained from the expanded anterior/lateral cristae area. **a** Schematic representation of the Type 5 experiment at the 10-somite stage, including the presumptive areas of the anterior and posterior ampullary cristae ($n=7$). **b–l** Horizontal sections through one Type 5 chimaeric embryo at E10. Grafted QCPN-positive cells were detected in the anterior and lateral cristae (between arrowheads in **b** and **c**). A large number of QN-positive dendrites were observed at the anterior crista (arrowheads in ac, **d**). QN-stained dendrites were detected also at the lateral crista (lc, **e**), the macula sacculi (ms, **h**) and the distal basilar papilla (*d*-bp, **k**). In contrast, the macula utriculi (mu, **g**), the intermediate basilar papilla (*i*-bp; **j**), the posterior crista (pc, **f** and **i**), the macula lagena (ml, **l**) and the macula neglecta (mn, **i**) presented few QN-stained processes. The proximal basilar papilla (not shown) was completely devoid of labelled quail dendrites. **m** Diagram summarising all these results. *M* medial, *R* rostral

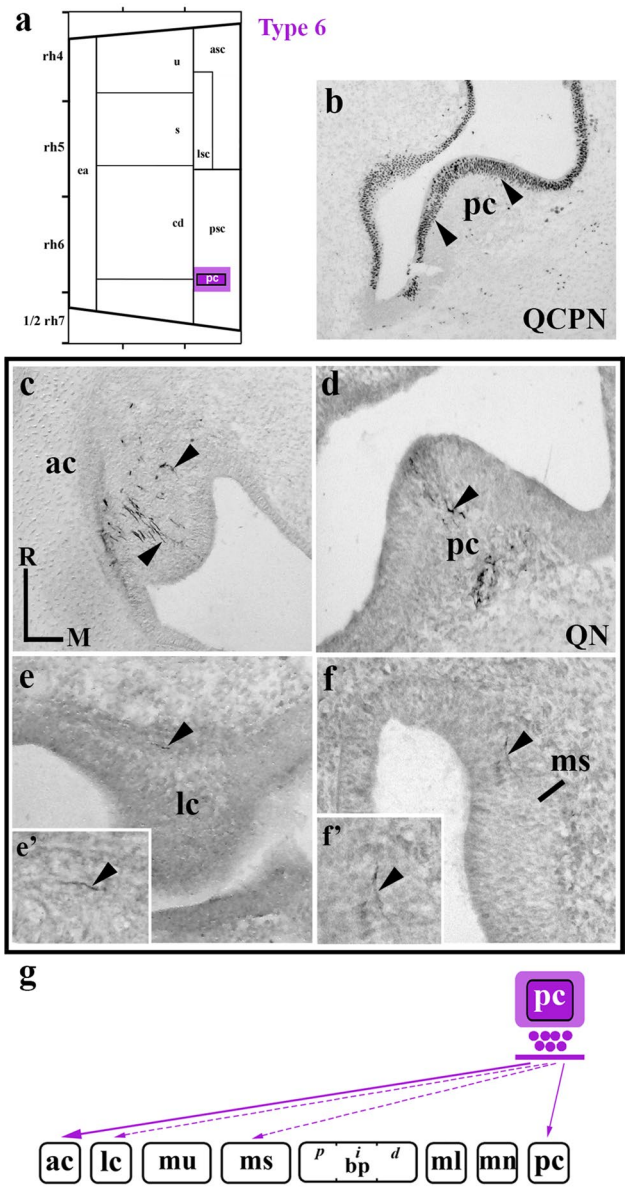

Fig. 9 Labelling obtained from the expanded posterior crista area. **a** Schematic representation of the Type 6 experiment at the 10-somite stage, involving the posterior crista area ($n=6$). **b–f** Horizontal sections through one Type 6 chimaeric embryo at E10. The posterior crista was the only sensory area included in the graft (between arrowheads in **b**). QN-positive fibres (arrowheads) were detected in the anterior and posterior cristae (ac, **c**; pc, **d**). A few QN-positive dendrites were observed in the lateral crista (pc, **e**, **e′**) and in the macula sacculi (ms, **f**, **f′**). **g** Diagram summarising all these results. *M* medial, *R* rostral

Neuroblasts derived from the expanded posterior crista area

Finally, the area of the presumptive posterior crista was selectively transplanted at stage HH10 (Type 6; pc in Fig. 9a and between arrowheads in Fig. 9b; see S6 Fig.). QN-positive processes were detected in the anterior crista (ac, Fig. 9c). Quail-derived neurons also innervated the posterior crista (pc, Fig. 9d). However, very few QN-positive dendrites, in some cases just one or two, were observed in the lateral crista (lc, Fig. 9e, e′) and macula sacculi (ms, Fig. 9f, f′). The other otic sensory patches were totally devoid of QN-stained fibres (not shown). Figure 9g summarises these results (see also Table 1).

Table 1 is a synthesis of the results for all the chimaeric embryos analysed, covering from Type 1 to Type 6 experiments, including a quantitative study of the area of each sensory element innervated by grafted neurons in type of experiment. Three, two and one asterisks correspond to thick, intermediate and thin arrows, respectively, which are shown in separate figures for each grafted region (Figs. 4l, 5m, 6l, 7m, 8m, 9g). When less than three QN-stained axons were detected within a sensory patch, a thin broken line is used (Fig. 9g).

Discussion

Neurogenesis at otic placode/cup stages

Otic neuroblast specification is the first cell differentiation to take place in the developing inner ear (Adam et al. 1998; Alsina et al. 2003, 2004, 2009; Abello and Alsina 2007; Bell et al. 2008; Vázquez-Echeverría et al. 2008; Wu and Kelley 2012; Lassiter et al. 2014; Raft and Groves 2015; see Introduction). *Fgf10* expression was observed in the anteromedialmost portion of the otic placode (stage HH10) and the early otic cup (stages 11–12), anticipating the pan-sensory competent territory (Alsina et al. 2004). In the chick, analysis of neural determination markers has shown a direct relationship between this pan-sensory *Fgf10*-expressing domain and otic neurogenesis (Alsina et al. 2004, 2009; Abelló et al. 2007; Bell et al. 2008). Although a different dynamic expression pattern of the *Fgf10* gene has been reported in the developing otic epithelium of mouse embryos, probably a reflection of different mechanisms of otic patch specification among vertebrate species, *Fgf10* expression is also clearly detected in the delaminating neuroblasts of the forming mammalian acoustic–vestibular ganglion (Pauley et al. 2003). It is generally accepted that *Neurogenin-1* (*Neurog1*) is an excellent otic neuronal determination gene (Ma et al. 1998, 2000). It belongs to an ancient family of basic Helix–Loop–Helix (bHLH) genes which are directly involved in cell fate determination across diverse phyla and neural systems (Alsina et al. 2009; Fritzsch et al. 2010). *Neurog1* expression is also confined to the anterior half of the otic cup (Alsina et al. 2004; Vázquez-Echeverría et al. 2008), within the *Fgf10*-expressing domain (Alsina et al. 2004) in an area probably corresponding to the future utricular and

saccular maculae and likely including some ampullary cristae (Bell et al. 2008; Sánchez-Guardado et al. 2014). In addition, *NeuroD* and *NeuroM* are related bHLH transcription factors controlled by *Neurog1* (Ma et al. 1998). They are involved in the differentiation of pre-specified neuroblasts into mature neurons, as well as in neuronal migration and survival (Fritzsch et al. 2006; Alsina et al. 2009; Jahan et al. 2010). *NeuroD* and *NeuroM* expressions are first detected in a few cells of the anterolateralmost portion of the early otic cup (HH12), and extends towards the anteromedial portion somewhat later (HH13) (Alsina et al. 2004; Abelló et al. 2007; Bell et al. 2008; Vázquez-Echeverría et al. 2008), with *NeuroD1* being essential for neuroblast delamination (Liu et al. 2000). Interestingly, *NeuroD* and *NeuroM* expressions are detected in the entire *Fgf10*-expressing domain of the developing chick inner ear, albeit reaching the extreme posteromedial portion of the otic cup at a later stage (HH14) (Alsina et al. 2004). This is the site where the caudal sensory patches develop (Sánchez-Guardado et al. 2014). In the mouse, neurogenic events begin at the anteroposterior midline of the invaginating otic placode (Raft et al. 2004; Raft and Groves 2015). These descriptive studies, our previous fate mapping study (Sánchez-Guardado et al. 2014), and the present work grafting different small areas carrying distinct sensory elements of the avian otic placode make it conceivable that, apart from the utricle and saccule, other portions of the developing membranous labyrinth in which the presumptive domain of some sensory patches develops participate in otic neurogenesis.

Neurogenesis at the otic vesicle stage

The origin of all otic neuroblasts has been ascribed to the anteroventral wall of the otic vesicle (D'Amico-Martel 1982; Carney and Silver 1983; Alvarez et al. 1989), with this neurogenic area being defined by the expression of such markers as *Neurog1*, *Delta1*, *LFng* and *NeuroD* (Begbie et al. 2002; Matei et al. 2005; Raft et al. 2007; Koundakjian et al. 2007; Vázquez-Echeverría et al. 2008; Alsina et al. 2009; Puligilla et al. 2010; Radosevic et al. 2011; Wu and Kelley 2012; Sapède et al. 2012; Groves et al. 2013). Clonal fate mapping studies of the developing chick inner ear using a replication-defective retrovirus have shown AVG neurons and sensory cells in the utricular macula to share a common lineage (Satoh and Fekete 2005), and genetic fate mapping of the *Neurog1*-expressing cells in the mouse inner ear has provided evidence for a shared lineage of AVG neurons and the utricular and saccular maculae (Raft et al. 2007; Raft and Groves 2015). Koundakjian and co-workers (Koundakjian et al. 2007) have shown that early *Neurog1*-expressing cells give rise mainly to the vestibular ganglion, whereas the late *Neurog1*-expressing cells contribute to the cochlear ganglion (Koundakjian et al. 2007). Temporal coupling of the vestibular/acoustic neuronal and utricular/saccular macular fate specifications has been hypothesised (Deng and Wu 2016). However, the possibility of other areas participating in the generation of additional neuroblasts cannot be excluded. Interestingly, neurosensory lineage reconstruction by imaging zebrafish embryos in vivo has clearly shown the posterior expansion over time of the neuroblast delamination domain (Dyballa et al. 2017). Also in zebrafish embryos, in the posteromedial portion of the otic epithelium, there is a population of bipotent progenitors that generate sensory cells and neurons, and in these progenitors, *neurog1* prevents *atoh1* expression, whereas *neurod1* is directly involved in hair cell fate specification (Sapède et al. 2012).

Islet1-positive neuroblasts delaminate from the ventral pole of the chick otic vesicle (Alsina et al. 2004; Raft et al. 2004; Li et al. 2004; Radde-Gallwitz et al. 2004). In this respect, it is well accepted that at least the auditory sensory organ and the corresponding ganglion neurons develop from this ventral area (Radde-Gallwitz et al. 2004; Raft and Groves 2015). Furthermore, the transcription factor *Prox1* is implicated in sensory and neural cell fates in the chick inner ear (Stone et al. 2003). Although delamination of *cProx1*-positive cells from the dense *cProx1*-expressing domain is not easily observed, *cProx1* expression is clearly detected at the medial edge of the anterior dense region at stage 21 (Stone et al. 2003), probably corresponding to a small non-sensory domain located between the anterior/lateral cristae and the macula utriculi. Interestingly, scattered *Prox1*-/Tuj1(βIII-tubuline)-positive cells are found within a continuous anteroventral-to-posteromedial band of the otic sensory anlagen, and they clearly migrate into the AVG primordium at the otocyst stage (Stone et al. 2003). In addition, analysis of *Fgf19* expression has also shown a possible delamination of otic neuroblasts far from the anteroventral portion of the otic vesicle, in an area corresponding to the presumptive territory of the posterior crista (Sanchez-Calderon et al. 2007a, b). The analysis of all the expanded sensory elements in early stages performed in this work and these previous findings clearly suggest the existence of distinct neurogenic areas in the developing inner ear, beyond the more precocious presumptive anteroventral territories (Koundakjian et al. 2007; Raft et al. 2007; Liu et al. 2000; Fariñas et al. 2001; Yang et al. 2011; Satoh and Fekete 2005).

Otic neurogenesis study in the developing avian inner ear using the quail/chick chimaeric graft method

In sum, various pieces of evidence point to multiple sites of delamination of otic neuroblasts from the developing membranous labyrinth over an extended period of time (from the

early otic cup stage onwards). These studies confirm that otic neurogenesis takes place intensely within an anteroventral part of the pan-sensory domain, in particular the presumptive territories of the utricular and saccular maculae (Satoh and Fekete 2005; Raft et al. 2007; Raft and Groves 2015). They lend powerful support to the assumption that neurogenesis also occurs within the auditory organ (Fariñas et al. 2001; Yang et al. 2011). However, there has yet to be full verification of the conjectured existence of multiple sites of otic neurogenesis within the developing membranous labyrinth, in particular, the presumptive territories of the cristae and the rest of the maculae in birds, and certainly in some adjacent non-sensory domains. Our results contribute to shedding light on this question, although the grafting experiments do not allow to determinate the neuroblasts generation time or their clonal relationship with hair cells from the sensory patch where they delaminated. We have analysed experimentally the origin of neuroblasts from diverse fate-mapped sites of the avian otic epithelium. When small portions of the otic placode containing the presumptive territory of sensory patches plus contiguous non-sensory epithelium were grafted homotopically (Sánchez-Guardado et al. 2014), the resulting chimaeric embryos showed that all the developing expanded sensory areas generate QCPN-positive neuroblast populations (Table 1). Two possible explanations could be considered: (1) all grafted areas contain small portions of the previously described neurogenic domain at stage HH10, and neuroblasts are generated early before sensory commitment is established; and/or (2) the grafted territory, containing the presumptive territory of sensory patches plus their contiguous non-sensory epithelium, activates neurogenesis at later points in development than those considered in previous work, thus leading to some subpopulations of otic neuroblasts being missed in the studies. The present results fit well with a previous DiI/DiO fate map study (Bell et al. 2008).

At the otic vesicle stage, it is also well known that otic neurogenesis occurs within a large sensory-competent domain of the otic rudiment defined by the overlapping expression of such pan-sensory markers as *Fgf10*, *Serrate1* and *Sox2* (Raft and Groves 2015). In chick embryos, *Fgf10* transcripts are present initially in a narrow ventromedial band of the otocyst, extending from its rostral to its caudal poles (Alsina et al. 2004; Sánchez-Guardado et al. 2013). Studies of the expression pattern of Islet1, a LIM-HD protein and *Fgf19* suggest that relevant otic neurogenesis occurs at the interface between the *Fgf10*-positive pan-sensory and the *Fgf10*-negative non-sensory domains (Alsina et al. 2004; Sanchez-Calderon et al. 2007a, b), suggesting that compartmentalization of the developing membranous labyrinth could be involved in otic neurogenesis (Fekete and Wu 2002; Alsina et al. 2004, 2009; Raft and Groves 2015). The grafted areas analysed in this work could contain part of the narrow neurogenic band overlapping the pan-sensory *Fgf10*-expressing domain and the non-sensory domains at the otic vesicle stage. As development proceeds, the *Fgf10*-expressing area observed in the otic vesicle splits repeatedly into several separate sub-areas, creating six of the eight sensory organs present in birds. Only the lateral crista and the macula neglecta are initially *Fgf10* negative, although they activate *Fgf10* expression after their specification as sensory elements (Sánchez-Guardado et al. 2013). The grafts performed in the present work contain one, or in some cases two, of these specified *Fgf10*-positive sensory patches plus contiguous areas of their respective non-sensory epithelia, together termed here "expanded presumptive sensory areas". It was not possible to determine whether grafted neuroblasts arose exclusively from either the sensory patch or the nearby non-sensory grafted area, or even from the interface between them. Further work would seem to be required to resolve this question.

Sensorial innervation pattern study in the developing avian inner ear using the quail/chick chimaeric graft method

Using a QN immunoreaction, which allows us to visualise the quail ganglionic dendrites approaching the quail or chicken otic sensory patches, we determined the sensory connection patterns generated by diverse graft-derived neurons. With respect to the macular areas, our study clearly showed that the expanded macula utriculi area, which contains the topologically rostral most macula, generated many neuroblasts, and that their dendrites reached every sensory patch (Type 1 graft). The macula sacculi area, fate mapped just caudal to the macula utriculi in the chicken otic placode, also generated many neuroblasts with indiscriminate connections (Type 2 graft). Interestingly, expanded grafts including the presumptive basilar papilla area (Type 3 graft), located even more caudally in the placode, produced fewer neuroblast, although still an appreciable number of them. In these last two types of graft (Types 2 and 3), the proximal portion of the basilar papilla was the only sensory domain devoid of QN-grafted dendrites. It is the first time reported that the caudalmost macular area, the macula lagena and the macula neglecta also generated neuroblasts when they were grafted (Type 4 graft). There were fewer of these Type 4-derived neuroblasts than those deriving from the basilar papillary area, and hence also far fewer than those from the utricular and saccular macular areas. Interestingly, quail neuron processes from Type 4-grafted neuroblasts still innervated, although to a lesser extent, all sensory patches.

A curious finding was that the proximal and intermediate portions of the basilar papilla never received dendritic contacts from the lagenar and neglecta macular grafted areas. A pattern of gradually emerging tonotopic projection to the

basilar papilla was discernible, with the rostralmost macular area (mu) differentiating earlier during development, and first projecting to the whole basilar papilla and the other more caudal macular areas (ms, ml and mn), differentiating later, and finally projecting exclusively to the caudalmost portion. These differences in the innervation pattern could also be related to the apex-base gradient of cellular differentiation and the innervation pattern of the developing organ of Corti (Xiang et al. 2003; Matei et al. 2005; Nichols et al. 2008; Yang et al. 2011; Wu and Kelley 2012; Kersigo and Fritzsch 2015; Dvorakova et al. 2016; Liu et al. 2016), as well as to the final tonotopic projections that connect a given position of the auditory sensory organ with the cochlear nuclei in the hindbrain (Rubel and Fritzsch 2002).

Regarding the crista-related areas, whose primordia are also aligned along the AP dimension of the placode, the anterior and lateral cases (Type 5 graft) clearly generated ganglionic neuroblasts that likewise innervated all otic sensory elements, except apparently the proximal portion of the basilar papilla. The expanded posterior crista area (Type 6 graft) generated comparatively fewer neuroblasts, which mainly innervated the anterior and posterior cristae and, to a far lesser extent, the lateral crista and the macula sacculi. The analysis of QN-positive processes of the neuroblasts from the expanded crista-related placodal areas is, thus, indicative of a differential connection of the dendrites from rostral versus caudal neuroblasts to the basilar papilla, as well as to other sensory patches.

In conclusion, our results have shown that: (1) neuroblasts from a small grafted area of the chick otic placode never exclusively connect with the correlative grafted sensory patch, but also with various other topologically distant areas; (2) the assumption that innervation of the developing inner ear is determined by lineage relationships between locally derived neurons and sensory cells clearly appears to be questionable, and (3) Although each expanded presumptive sensory area can generate neuroblasts, the "reverse-pathfinding" mechanism by which pioneering dendritic processes return specifically to given sensory organs following the original migratory paths of the neuroblast ought to be completely discarded from further consideration as a realistic description of otic dendritic guidance. The focus of more advanced studies should address the possible existence of a non-specific general chemoattractant for ganglionic dendrites that is released by all sensory patches, probably in a rostrocaudal spatiotemporal sequence. One has to assume that the indiscriminate primary innervation pattern that has been demonstrated here will undergo processes of correction at later stages, eliminating redundant connections, and finally establishing the highly selective innervation pattern described in adult animals (Echteler 1992; Delacroix and Malgrange 2015). There are various plausible factors that may lead to such significant synaptic refining. They reduce the efficiency of the postulated generic attractant as the size of the labyrinth grows, the possible later production of more selective attractants as the sensory patches differentiate, competition among redundant contacts and application of "the first to arrive takes all" rule, receive sensory input and trophic effects due to functional mismatch in the axonal projections of the ganglionic neurons into the corresponding hindbrain sensory columns.

Acknowledgements We express our gratitude to Dr Tanaka for providing us with QN antibodies.

Author contributions MH-S, L-OS-G and LP designed experiments. L-OS-G and MH-S performed experiments. MH-S, L-OS-G and LP analysed data and wrote the manuscript.

Funding This work was supported by the following Grant sponsors: Spanish Ministry of Science, BFU2010-1946; Junta de Extremadura, GR10152, GR15158 and IB18046 (to M.H.-S.); Spanish MICINN Grant BFU2014-57516P; SENECA Foundation contract 19904/GERM/15 (to L.P.); Junta de Extremadura pre-doctoral studentshipvaage; Grant number PRE/08031 (to L.-O.S.-G.).

Compliance with ethical standards

Conflict of interest The authors declare that they have no conflict of interest.

Ethical approval All procedures performed in studies involving animals were in accordance with the ethical standards of the institution or practice where the studies were conducted.

Informed consent Informed consent was obtained from all individual participants included in the study.

References

Abello G, Alsina B (2007) Establishment of a proneural field in the inner ear. Int J Dev Biol 51:483–493

Abelló G, Khatri S, Giráldez F, Alsina B (2007) Early regionalization of the otic placode and its regulation by the Notch signaling pathway. Mech Dev 124:631–645

Adam J, Myat A, Le Roux I, Eddison M, Henrique D, Ish-Horowicz D, Lewis J (1998) Cell fate choices and the expression of Notch, Delta and Serrate homologues in the chick inner ear: parallels with Drosophila sense-organ development. Development 125:4645–4654

Alsina B, Whitfield TT (2017) Sculpting the labyrinth: morphogenesis of the developing inner ear. Semin Cell Dev Biol 65:47–59

Alsina B, Giraldez F, Varela-Nieto I (2003) Growth factors and early development of otic neurons: interactions between intrinsic and extrinsic signals. Curr Top Dev Biol 57:177–206

Alsina B, Abelló G, Ulloa E, Henrique D, Pujades C, Giraldez F (2004) FGF signaling is required for determination of otic neuroblasts in the chick embryo. Dev Biol 267:119–134

Alsina B, Giraldez F, Pujades C (2009) Patterning and cell fate in ear development. Int J Dev Biol 53:1503–1513

Alvarado-Mallart RM, Sotelo C (1984) Homotopic and heterotopic transplantations of quail tectal primordia in chick embryos:

organization of the retinotectal projections in the chimeric embryos. Dev Biol 103:378–398
Alvarez IS, Martín-Partido G, Rodríguez-Gallardo L, González-Ramos C, Navascués J (1989) Cell proliferation during early development of the chick embryo otic anlage: quantitative comparison of migratory and nonmigratory regions of the otic epithelium. J Comp Neurol 290:278–288
Begbie J, Ballivet M, Graham A (2002) Early steps in the production of sensory neurons by the neurogenic placodes. Mol Cell Neurosci 21:502–511
Beisel KW, Wang-Lundberg Y, Maklad A, Fritzsch B (2005) Development and evolution of the vestibular sensory apparatus of the mammalian ear. J Vestib Res 15:225–241
Bell D, Streit A, Gorospe I, Varela-Nieto I, Alsina B, Giraldez F (2008) Spatial and temporal segregation of auditory and vestibular neurons in the otic placode. Dev Biol 322:109–120
Bermingham NA, Hassan BA, Price SD, Vollrath MA, Ben-Arie N, Eatock RA, Bellen HJ, Lysakowski A, Zoghbi HY (1999) Math1: an essential gene for the generation of inner ear hair cells. Science 284:1837–1841
Bok J, Chang W, Wu DK (2007) Patterning and morphogenesis of the vertebrate inner ear. Int J Dev Biol 51:521–533
Carney PR, Silver J (1983) Studies on cell migration and axon guidance in the developing distal auditory system of the mouse. J Comp Neurol 215:359–369
Chen J, Streit A (2013) Induction of the inner ear: stepwise specification of otic fate from multipotent progenitors. Hear Res 297:3–12
Coate TM, Kelley MW (2013) Making connections in the inner ear: recent insights into the development of spiral ganglion neurons and their connectivity with sensory hair cells. Semin Cell Dev Biol 24:460–469
Coate TM, Spita NA, Zhang KD, Isgrig KT, Kelley MW (2015) Neuropilin-2/Semaphorin-3F-mediated repulsion promotes inner hair cell innervation by spiral ganglion neurons. Elife 4
D'Amico-Martel A (1982) Temporal patterns of neurogenesis in avian cranial sensory and autonomic ganglia. Am J Anat 163:351–372
D'Amico-Martel A, Noden DM (1983) Contributions of placodal and neural crest cells to avian cranial peripheral ganglia. Am J Anat 166:445–468
Delacroix L, Malgrange B (2015) Cochlear afferent innervation development. Hear Res 330:157–169
Deng X, Wu DK (2016) Temporal coupling between specifications of neuronal and macular fates of the inner ear. Dev Biol 414:21–33
Dvorakova M, Jahan I, Macova I, Chumak T, Bohuslavova R, Syka J, Fritzsch B, Pavlinkova G (2016) Incomplete and delayed Sox2 deletion defines residual ear neurosensory development and maintenance. Sci Rep 6:38253
Dyballa S, Savy T, Germann P, Mikula K, Remesikova M, Špir R, Zecca A, Peyriéras N, Pujades C (2017) Distribution of neurosensory progenitor pools during inner ear morphogenesis unveiled by cell lineage reconstruction. eLife 6:e22268
Echteler SM (1992) Developmental segregation in the afferent projections to mammalian auditory hair cells. PNAS 89:6324–6327
Elliott KL, Fritzsch B (2018) Ear transplantations reveal conservation of inner ear afferent pathfinding cues. Sci Rep 8:13819
Fariñas I, Jones KR, Tessarollo L, Vigers AJ, Huang E, Kirstein M, de Caprona DC, Coppola V, Backus C, Reichardt LF, Fritzsch B (2001) Spatial shaping of cochlear innervation by temporally regulated neurotrophin expression. J Neurosci 21:6170–6180
Fekete DM, Campero AM (2007) Axon guidance in the inner ear. Int J Dev Biol 51:549–556
Fekete DM, Wu DK (2002) Revisiting cell fate specification in the inner ear. Curr Opin Neurobiol 12:35–42
Freyer L, Aggarwal V, Morrow BE (2011) Dual embryonic origin of the mammalian otic vesicle forming the inner ear. Development 138:5403–5414
Fritzsch B (1993) Fast axonal diffusion of 3000 molecular weight dextran amines. J Neurosci Methods 50:95–103
Fritzsch B (2003) Development of inner ear afferent connections: forming primary neurons and connecting them to the developing sensory epithelia. Brain Res Bull 60:423–433
Fritzsch B, Beisel KW, Jones K, Fariñas I, Maklad A, Lee J, Reichardt LF (2002) Development and evolution of inner ear sensory epithelia and their innervation. J Neurobiol 53:143–156
Fritzsch B, Tessarollo L, Coppola E, Reichardt LF (2004) Neurotrophins in the ear: their roles in sensory neuron survival and fiber guidance. Prog Brain Res 146:265–278
Fritzsch B, Pauley S, Matei V, Katz DM, Xiang M, Tessarollo L (2005) Mutant mice reveal the molecular and cellular basis for specific sensory connections to inner ear epithelia and primary nuclei of the brain. Hear Res 206:52–63
Fritzsch B, Pauley S, Beisel KW (2006) Cells, molecules and morphogenesis: the making of the vertebrate ear. Brain Res 1091:151–171
Fritzsch B, Eberl DF, Beisel KW (2010) The role of bHLH genes in ear development and evolution: revisiting a 10-year-old hypothesis. Cell Mol Life Sci 67:3089–3099
Fritzsch B, Pan N, Jahan I, Elliott KL (2015) Inner ear development: building a spiral ganglion and an organ of Corti out of unspecified ectoderm. Cell Tissue Res 361:7–24
Gálvez H, Abelló G, Giraldez F (2017) Signaling and Transcription factors during inner ear development: the generation of hair cells and otic neurons. Front Cell Dev Biol 5:21
Groves AK, Fekete DM (2012) Shaping sound in space: the regulation of inner ear patterning. Development 139:245–257
Groves AK, Zhang KD, Fekete DM (2013) The genetics of hair cell development and regeneration. Annu Rev Neurosci 36:361–381
Hamburger V, Hamilton HL (1992) A series of normal stages in the development of the chick embryo. 1951. Dev Dyn 195:231–272
Hemond SG, Morest DK (1991) Ganglion formation from the otic placode and the otic crest in the chick embryo: mitosis, migration, and the basal lamina. Anat Embryol 184:1–13
Hemond SG, Morest DK (1992) Tropic effects of otic epithelium on cochleo-vestibular ganglion fiber growth in vitro. Anat Rec 232:273–284
Holt JC, Lysakowski A, Goldberg JM (2011) The efferent vestibular system. In: Ryugo DK, Fay RR (eds) Auditory and vestibular efferents. Springer, New York, pp 135–186
Jahan I, Kersigo J, Pan N, Fritzsch B (2010) Neurod1 regulates survival and formation of connections in mouse ear and brain. Cell Tissue Res 341:95–110
Kawamoto K, Ishimoto S-I, Minoda R, Brough DE, Raphael Y (2003) Math1 gene transfer generates new cochlear hair cells in mature guinea pigs in vivo. J Neurosci 23:4395–4400
Kersigo J, Fritzsch B (2015) Inner ear hair cells deteriorate in mice engineered to have no or diminished innervation. Front Aging Neurosci 7:33
Koundakjian EJ, Appler JL, Goodrich LV (2007) Auditory neurons make stereotyped wiring decisions before maturation of their targets. J Neurosci 27:14078–14088
Lassiter RNT, Stark MR, Zhao T, Zhou CJ (2014) Signaling mechanisms controlling cranial placode neurogenesis and delamination. Dev Biol 389:39–49
Li H, Liu H, Sage C, Chen ZY, Heller S (2004) Islet-1 expression in the developing chicken inner ear. J Comp Neurol 477:1–10
Liu M, Pereira FA, Price SD, Chu MJ, Shope C, Himes D, Eatock RA, Brownell WE, Lysakowski A, Tsai MJ (2000) Essential role of BETA2/NeuroD1 in development of the vestibular and auditory systems. Genes Dev 14:2839–2854
Liu H, Li Y, Chen L, Zhang Q, Pan N, Nichols DH, Zhang WJ, Fritzsch B, He DZ (2016) Organ of corti and stria vascularis: is there an Interdependence for survival? PLoS One 11:e0168953

Ma Q, Chen Z, del Barco Barrantes I, de la Pompa JL, Anderson DJ (1998) neurogenin1 is essential for the determination of neuronal precursors for proximal cranial sensory ganglia. Neuron 20:469–482

Ma Q, Anderson DJ, Fritzsch B (2000) Neurogenin 1 null mutant ears develop fewer, morphologically normal hair cells in smaller sensory epithelia devoid of innervation. J Assoc Res Otolaryngol 1:129–143

Mahmoud A, Reed C, Maklad A (2013) Central projections of lagenar primary neurons in the chick. J Comp Neurol 521:3524–3540

Maklad A, Fritzsch B (2003) Development of vestibular afferent projections into the hindbrain and their central targets. Brain Res Bull 60:497–510

Maklad A, Kamel S, Wong E, Fritzsch B (2010) Development and organization of polarity-specific segregation of primary vestibular afferent fibers in mice. Cell Tissue Res 340:303–321

Mao Y, Reiprich S, Wegner M, Fritzsch B (2014) Targeted deletion of Sox10 by Wnt1-cre defects neuronal migration and projection in the mouse inner ear. PLoS One 9:e94580

Matei V, Pauley S, Kaing S, Rowitch D, Beisel KW, Morris K, Feng F, Jones K, Lee J, Fritzsch B (2005) Smaller inner ear sensory epithelia in Neurog 1 null mice are related to earlier hair cell cycle exit. Dev Dyn 234:633–650

Meas SJ, Zhang C-L, Dabdoub A (2018) Reprogramming glia into neurons in the peripheral auditory system as a solution for sensorineural hearing loss: lessons from the central nervous system. Front Mol Neurosci 11:77

Nichols DH, Pauley S, Jahan I, Beisel KW, Millen KJ, Fritzsch B (2008) Lmx1a is required for segregation of sensory epithelia and normal ear histogenesis and morphogenesis. Cell Tissue Res 334:339–358

Noden DM, van de Water T (1986) The developing ear: tissue origins and interactions. Biol Change Otolaryngol 15–46

Pauley S, Wright TJ, Pirvola U, Ornitz D, Beisel K, Fritzsch B (2003) Expression and function of FGF10 in mammalian inner ear development. Dev Dyn 227:203–215

Puligilla C, Dabdoub A, Brenowitz SD, Kelley MW (2010) Sox2 induces neuronal formation in the developing mammalian cochlea. J Neurosci 30:714–722

Radde-Gallwitz K, Pan L, Gan L, Lin X, Segil N, Chen P (2004) Expression of Islet1 marks the sensory and neuronal lineages in the mammalian inner ear. J Comp Neurol 477:412–421

Radosevic M, Robert-Moreno A, Coolen M, Bally-Cuif L, Alsina B (2011) Her9 represses neurogenic fate downstream of Tbx1 and retinoic acid signaling in the inner ear. Development 138:397–408

Raft S, Groves AK (2015) Segregating neural and mechanosensory fates in the developing ear: patterning, signaling, and transcriptional control. Cell Tissue Res 359:315–332

Raft S, Nowotschin S, Liao J, Morrow BE (2004) Suppression of neural fate and control of inner ear morphogenesis by Tbx1. Development 131:1801–1812

Raft S, Koundakjian EJ, Quinones H, Jayasena CS, Goodrich LV, Johnson JE, Segil N, Groves AK (2007) Cross-regulation of Ngn1 and Math1 coordinates the production of neurons and sensory hair cells during inner ear development. Development 134:4405–4415

Rubel EW, Fritzsch B (2002) Auditory system development: primary auditory neurons and their targets. Annu Rev Neurosci 25:51–101

Sanchez-Calderon H, Milo M, Leon Y, Varela-Nieto I (2007) A network of growth and transcription factors controls neuronal differentation and survival in the developing ear. Int J Dev Biol 51:557–570

Sánchez-Calderón H, Francisco-Morcillo J, Martín-Partido G, Hidalgo-Sánchez M (2007) Fgf19 expression patterns in the developing chick inner ear. Gene Expr Patterns 7:30–38

Sánchez-Guardado LO, Ferran JL, Mijares J, Puelles L, Rodríguez-Gallardo L, Hidalgo-Sánchez M (2009) Raldh3 gene expression pattern in the developing chicken inner ear. J Comp Neurol 514:49–65

Sánchez-Guardado LÓ, Puelles L, Hidalgo-Sánchez M (2013) Fgf10 expression patterns in the developing chick inner ear. J Comp Neurol 521:1136–1164

Sánchez-Guardado LÓ, Puelles L, Hidalgo-Sánchez M (2014) Fate map of the chicken otic placode. Development 141:2302–2312

Sapède D, Dyballa S, Pujades C (2012) Cell lineage analysis reveals three different progenitor pools for neurosensory elements in the otic vesicle. J Neurosci 32:16424–16434

Satoh T, Fekete DM (2005) Clonal analysis of the relationships between mechanosensory cells and the neurons that innervate them in the chicken ear. Development 132:1687–1697

Schneider-Maunoury S, Pujades C (2007) Hindbrain signals in otic regionalization: walk on the wild side. Int J Dev Biol 51:495–506

Simmons D, Duncan J, de Caprona DC, Fritzsch B (2011) Development of the inner ear efferent system. In: Ryugo DK, Fay RR (eds) Auditory and vestibular efferents. Springer, New York, pp 187–216

Stevens CB, Davies AL, Battista S, Lewis JH, Fekete DM (2003) Forced activation of Wnt signaling alters morphogenesis and sensory organ identity in the chicken inner ear. Dev Biol 261:149–164

Stone JS, Shang J-L, Tomarev S (2003) Expression of Prox1 defines regions of the avian otocyst that give rise to sensory or neural cells. J Comp Neurol 460:487–502

Straka H, Baker R (2013) Vestibular blueprint in early vertebrates. Front Neural Circuits 7:182

Tanaka H, Kinutani M, Agata A, Takashima Y, Obata K (1990) Pathfinding during spinal tract formation in the chick-quail chimera analysed by species-specific monoclonal antibodies. Development 110:565–571

Vaage S (1969) The segmentation of the primitive neural tube in chick embryos (*Gallus domesticus*). A morphological, histochemical and autoradiographical investigation. Ergeb Anat Entwicklungsgesch 41:3–87

Vázquez-Echeverría C, Dominguez-Frutos E, Charnay P, Schimmang T, Pujades C (2008) Analysis of mouse kreisler mutants reveals new roles of hindbrain-derived signals in the establishment of the otic neurogenic domain. Dev Biol 322:167–178

Whitfield TT, Hammond KL (2007) Axial patterning in the developing vertebrate inner ear. Int J Dev Biol 51:507–520

Wu DK, Kelley MW (2012) Molecular mechanisms of inner ear development. Cold Spring Harb Perspect Biol 4:a008409

Xiang M, Maklad A, Pirvola U, Fritzsch B (2003) Brn3c null mutant mice show long-term, incomplete retention of some afferent inner ear innervation. BMC Neurosci 4:2

Yang T, Kersigo J, Jahan I, Pan N, Fritzsch B (2011) The molecular basis of making spiral ganglion neurons and connecting them to hair cells of the organ of Corti. Hear Res 278:21–33

Zhang KD, Coate TM (2017) Recent advances in the development and function of type II spiral ganglion neurons in the mammalian inner ear. Semin Cell Dev Biol 65:80–87